Observation of Chaotic Particle Transport Induced by Drift-Resonant Fluctuations in a Magnetic Dipole Field

H. P. Warren and M. E. Mauel

Department of Applied Physics, Columbia University, New York, New York 10027

(Received 5 May 1994)

The chaotic radial transport of energetic electrons trapped in a magnetic dipole field has been observed in a laboratory terrella. This transport is driven by multimode, drift-resonant plasma instabilities which are excited by the hot electron population. A transport simulation of energetic electrons interacting with a spectrum of electrostatic waves modeled on the measured fluctuations reproduces temporal features of the experimentally observed radial particle flux.

PACS numbers: 52.25.Fi, 52.35.–g, 94.20.Rr

Charged particles trapped in a dipole magnetic field undergo collisionless radial transport when nonaxisymmetric fluctuations break the third adiabatic invariant ψ, which is proportional to the unperturbed magnetic flux. For example, random variations in the solar wind intensity produce perturbations of the Earth's geomagnetic and convection electric fields which have a broad fluctuation spectrum dominated by low-order azimuthal components [1]. Quasilinear models of the resulting transport have been used to account for the radial profile of radiation belt particles measured with satellites [2,3]. The more general problem of chaotic radial transport driven by nonlinear wave-particle resonances in a dipole magnetic field has been examined by Chan, Chen, and White [4] using Hamiltonian methods. For spectra characterized by multiple discrete modes, the extent of the transport is restricted both in radius and in energy by the existence of specific wave-particle resonances, and the transport need not be quasilinear [5]. Recently, these techniques have been used to study the time evolution of proton phase space distributions in the Earth's magnetosphere induced by a given fluctuation spectrum [6].

In this Letter, we report the first observations of wave-induced chaotic radial transport in a laboratory terrella, the Collisionless Terrella Experiment (CTX). These observations demonstrate a clear relationship between the wave spectrum and the induced resonant transport and provide the first laboratory test of Hamiltonian methods which can used to simulate magnetospheric transport. In addition, we observe wave-particle dynamics in an evolving nonlinear system which is a topic important to transport studies in other magnetically confined plasmas [7].

In CTX, an energetic population of trapped electrons is produced using electron cyclotron resonance heating (ECRH) [8]. The trapped electrons excite quasiperiodic "bursts" of drift-resonant instabilities which we identify as the hot electron interchange mode [9,10]. We find that during these bursts the measured amplitudes, frequencies, and azimuthal mode numbers of the drift-resonant fluctuations meet the conditions required for global chaotic particle transport. During these times, significantly enhanced electron transport is observed with a gridded particle detector and this transport is strongly modulated at the drift frequency of the energetic electrons. At other times, when the instability wave spectrum does not satisfy the conditions for global chaos, no enhanced transport is observed. A numerical simulation of trapped electrons interacting with electrostatic waves modeled on experimental measurements reproduces the modulation depth and frequency of the observed electron flux.

The experiments reported here differ significantly from laboratory terrella previously built to aid the understanding of global magnetospheric structure in the presence of a steady solar wind [11]. The CTX device does not have a "simulated" solar wind, and the low-density, hot electron plasmas produced in CTX are much less collisional than terrella experiments related to the solar wind. The experiments reported here also differ from the "collisionless" terrella experiments conducted in ultrahigh vacuum by Il'in and Il'ina [12]. They demonstrated the breakdown of the first two adiabatic invariants at high energy and observed a reduced adiabatic limit during the application of axisymmetric perturbations. In contrast, we study chaotic particle transport of an energetic belt of trapped electrons induced by low-frequency, nonaxisymmetric waves which preserve the first two adiabatic invariants [13].

The CTX device consists of a dipole magnet suspended mechanically within an aluminum vacuum vessel approximately 1.4 m in diameter. The plasma is created and heated by applying a 1 kW pulse of 2.54 GHz microwaves for approximately 1 sec. Just prior to and during the microwave pulse, hydrogen gas is puffed into the vacuum chamber to control the background neutral pressure. Typically, the initial pressure is ~ 0.3 μTorr and rises during the discharge depending on the duration and number of gas puffs. After a period lasting a few tenths of a second, a ring of hot trapped electrons forms near the flux surface containing the fundamental cyclotron resonance at the equatorial plane of the dipole. This hot electron population is similar to those created with ECRH in other magnetic traps [14]. Figure 1 shows the magnetic field geometry, the approximate location of the energetic electrons, and the representative placement of some of the probe diagnostics discussed below.

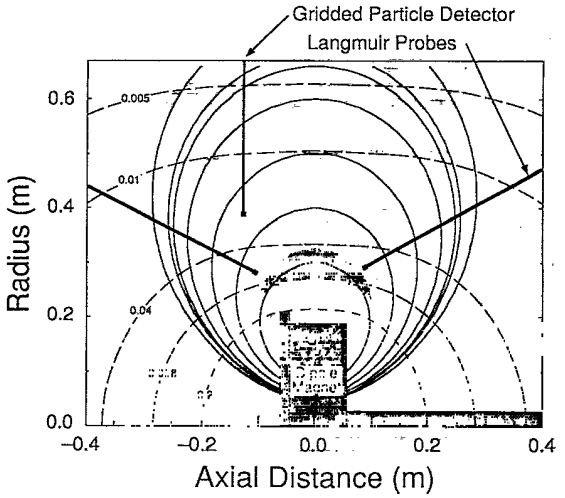

FIG. 1. Magnetic field lines (solid) and $|B|$ contours (dashed) in the CTX device. Heavy lines represent positions of movable probes. The shaded region indicates the approximate location of the energetic electron belt.

The characteristics of the energetic electrons are determined using a krypton proportional counter surrounded by a lead collimator aimed to view the equator of the dipole magnet. Bremsstrahlung emission at energies between 1 and 60 keV is recorded with a histogramming, multichannel analyzer every 50 msec. The energy and intensity of the emission are strongly dependent on the neutral hydrogen pressure. The most intense emission occurs when the pressure is ~ 3 μTorr. The observed distributions are non-Maxwellian, characteristic of microwave-heated electrons [14]. The electrons with energies between 1 and 10 keV are referred to as the "warm" population, and electrons with energies above 10 keV are referred to as the "hot" population. When the microwave power is switched off, the hot population persists for 5–20 msec, defining the discharge "afterglow."

The drift-resonant fluctuations are observed with Langmuir probes and high-impedance floating potential probes situated at five locations within the vacuum vessel. The probes can be repositioned radially to examine the density and potential fluctuations at different flux surfaces. Simultaneous measurements from multiple probes are used to determine the azimuthal mode number and radial mode structure of the fluctuations. We take the amplitude of the floating potential oscillations to be representative of the electrostatic oscillations of the plasma waves. Data from the probes are digitized using transient recorders capable of storing 2^{17} samples at rates of up to 100 MHz. The Langmuir probes are also used to estimate the spatial extent of the hot electron population since the x-ray emission is diminished as the probes contact the resonance region.

The transport of energetic electrons is detected with a movable, gridded particle detector. The detector is a cube with a width of 7 mm and with an angular acceptance of 1.5 sr. The grids are biased to repel ions and electrons with energies less than 100 eV, and the entrance aperture can be rotated with respect to the local magnetic field vector. For the measurements described here, the entrance was oriented perpendicular to the magnetic field excluding electrons with energies below approximately 3 keV due to gyroradius effects. Figure 1 shows the typical location of the gridded particle detector, slightly offset from the dipole's equatorial plane.

When an intense hot electron population is produced, drift-resonant fluctuations ($\omega \sim \omega_{dh}$) are observed both while the ECR heating is on and in the afterglow. During heating, the fluctuations occur in quasiperiodic bursts lasting approximately 300–500 μsec and having initial growth rate of $\sim 1/50$ μsec. The rate at which the bursts appear is a function of the hot electron intensity: at the highest observed energies the bursts become almost continuous, while at lower energies the interval between bursts increases. During the afterglow, the drift-resonant oscillations have a slower growth rate, $\sim 1/100$ μsec, and persist for several milliseconds. At both times, the observed instabilities propagate azimuthally in the direction of the electron ∇B drift, are flutelike with a constant phase along a field line, and have a broad radial structure extending throughout the plasma. The saturated amplitudes of the floating potential oscillations present at both times are also similar, typically 100–200 V, with the larger amplitudes resulting from the most energetic electron populations.

The time evolution of the spectral content of the waves was examined by computing the spectrogram of the potential fluctuations. Figure 2 shows the spectrogram of a floating potential probe signal taken at the end of the heating phase and extending into the afterglow. The quasiperiodic bursts consist of multiple frequencies typically below $f \leq 2$ MHz although some particularly intense bursts have reached frequencies as high as 5 MHz. These frequencies drift resonate with the warm electrons. The spectrogram also shows that the wave frequencies generally increase in time or "chirp." The rising tones are most evident during the intense coherent modes seen during the afterglow when the frequencies range from 1 to 10 MHz, resonating with the hot electrons. The chirp rate during the afterglow is sensitive to the intensity of the hot electrons: at high intensity the chirp rate is fast, and at lower intensities the rise in frequency is slower.

The Fourier transform of the correlation between Langmuir probes located at the same radius but separated in azimuth was computed in order to determine the azimuthal mode number of the various frequencies. The azimuthal mode number of the quasiperiodic bursts is usually limited to $m = 1$ except in the most intense bursts where modes with $m = 2$ are observed at high frequencies. During the afterglow $m \leq 6$ and several waves are observed simultaneously having the same m number.

We believe the drift-resonant fluctuations observed in CTX are related to the hot electron interchange

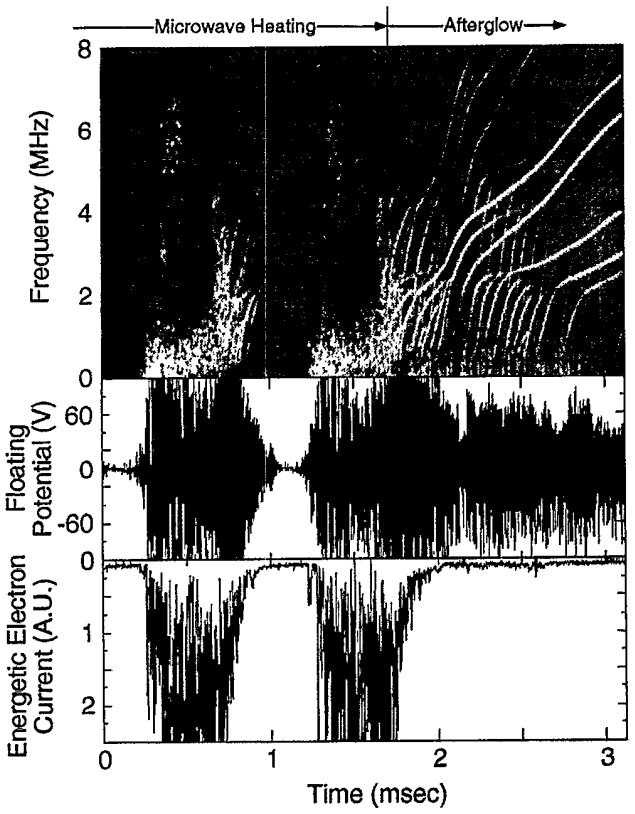

FIG. 2. Simultaneous measurements of drift-resonant fluctuations and energetic electrons near the end of the microwave heating pulse. Spectrogram (top) illustrates the multimode fluctuations with rising tones. Floating potential oscillations (middle) illustrate intense, quasiperiodic bursts correlated with rapid increase of electron flux (bottom) to the gridded particle detector.

instability (HEI) that has been observed in ECRH heated magnetic mirror experiments [8,15]. The linear dispersion relation for low-frequency ($\omega \ll \omega_{ci}$) electrostatic flute modes was developed by Krall [9] and extended to high-frequency modes ($\omega \sim \omega_{ci}$) by Berk [10]. These theories, which assume a monoenergetic distribution of hot electrons and slab geometry, predict instability when the energetic electron fraction exceeds some critical value.

When the linear theory is extended to include a distribution of velocities and dipole geometry, it predicts unstable modes with real frequency $\omega < m\bar{\omega}_{dh}/2$, where $\bar{\omega}_{dh}$ is the precessional drift frequency averaged over the distribution of energies. The fact that the real frequency of the instability is below the average drift frequency of the energetic electron population suggests a possible explanation of the chirping observed in the experiment. The instability drives transport in the lower energy particles first. The remaining distribution has a higher average energy which leads to a higher real frequency for the instability.

Coincident with the bursts of wave activity during ECRH, we observe increases in the flux of energetic electrons to the gridded particle detector indicating rapid radial transport. As shown in Fig. 2, the electron current rises significantly above the background level during the bursts. No transport is associated with the high-frequency wave activity observed in the afterglow. At this time, the measured wave spectrum produces isolated bands of stochastic radial motion not capable of global transport.

A feature of particular interest in Fig. 2 is the persistent modulation of the electron flux near the precessional drift frequency of the hot electrons. This type of behavior is suggestive of "drift echoes" which have been observed in satellite measurements of energetic particle transport [16]. Drift echoes result from the sudden injection of energetic particles at a narrow range of longitude. If the injected particles differ from the background population, each time they drift past the satellite a change in the particle flux is observed.

We conjecture that a similar process is responsible for the modulation of the observed particle flux in CTX. As we will show, the experimentally measured wave spectra are consistent with the observation of chaotic particle motion. The decorrelation time, however, is long with respect to a drift period. Thus inhomogeneities in phase space propagate azimuthally and lead to temporal variations in the particle flux.

The interaction of energetic electrons with the electrostatic waves observed in the experiment can be described by the guiding center drift Hamiltonian [17]

$$H = \tfrac{1}{2} m_e \rho_{\parallel}^2 B^2 + \mu B - e\Phi , \qquad (1)$$

where $\rho_{\parallel} \equiv v_{\parallel}/B$, and $\mu \equiv m_e v_{\perp}^2/2B$ is the first adiabatic invariant, the magnetic moment. The canonical variables, $(\rho_{\parallel}, \chi)$ and (ψ, φ), of the Hamiltonian are defined by $\mathbf{B} = \nabla\psi \times \nabla\varphi = \nabla\chi$, where $\psi = M\sin^2\theta/r$, $\chi = M\cos\theta/r^2$, $M \equiv B_0 R_0^3$ is the moment of the dipole magnet, and (r, φ, θ) are spherical coordinates. For simplicity, we examine only equatorial particles with $\rho_{\parallel} = \chi = 0$.

The fluctuations present during the quasiperiodic bursts are modeled as a sum of $m = 1$ fixed-frequency traveling waves,

$$\Phi(\varphi, t) = \sum_{l=1}^{N} \Phi_l \cos(\varphi - \omega_l t + \varphi_l) . \qquad (2)$$

The frequencies and relative amplitudes of the waves are taken directly from experimental observations. Each wave in the series forms a drift island of width $\Delta\psi_l \simeq (2e\Phi_l \psi_l^r/\omega_l)^{1/2}$, where ψ_l^r is the resonant surface defined by $\omega_d(\psi_l^r) = \omega_l$. When multiple drift-resonant waves have sufficiently large amplitudes, the islands will overlap and lead to chaotic transport [4]. This condition for chaos is visualized by constructing a Poincaré surface of section by plotting particle coordinates, (ψ, φ), at multiples of the mapping time defined by the least common multiple of the periods of the wave motion [18].

For a series of waves modeled on the initial part of an instability burst, drift resonances exist for electrons with energies between 3 and 10 keV (i.e., the warm electrons) from the center of the hot electron ring to the wall of

the vacuum chamber. Examination of the phase space portraits indicates that when the wave amplitude is above 75 V there are no encircling Kolmogorov-Arnol'd-Moser (KAM) surfaces preventing global transport. This implies that for the wave spectra measured in the experiment the conditions for chaotic particle transport are met.

In order to demonstrate the relationship between the modulation of the current and the spectral content of the observed fluctuations, we have simulated the time evolution of the flux of electrons to a small region of phase space which represents the particle detector. In the simulation, we randomly selected an ensemble of 5000 particle trajectories that are at the "gridded particle detector" at time $t = T$. Using spectral information from the experiment to construct the electrostatic potential in the form of Eq. (2), the equations of motion are integrated backwards in time from $t = T$ to $t = 0$, and the probability that the trajectory came from an assumed hot electron distribution, $F_h(\mu, \psi)$, is computed. This process is repeated in order to compute the current as a function of time.

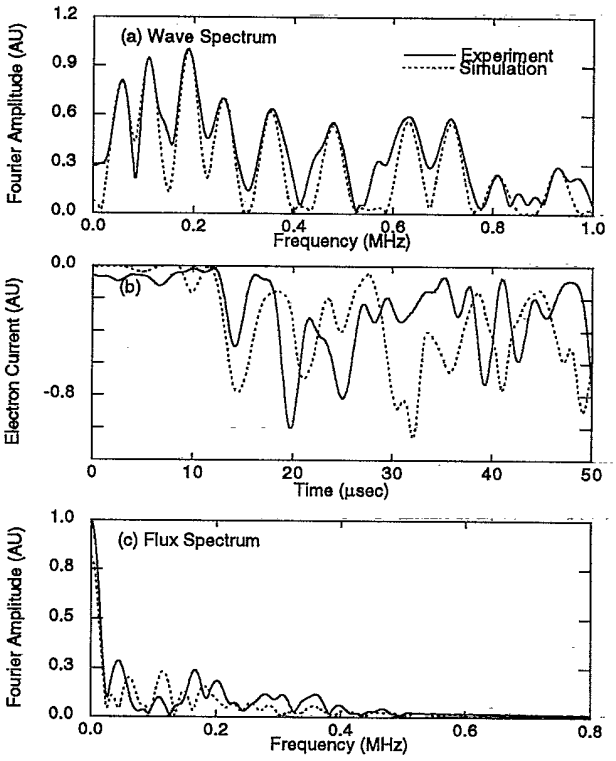

FIG. 3. A comparison of experiment and a simulation which reproduces the gross frequency and depth of the modulation. (a) Frequency spectrum of the electrostatic waves, (b) detected energetic electron flux, and (c) Fourier transform of the detected flux.

The result of one such simulation is presented in Fig. 3. Here the frequency spectrum, the energetic electron flux to the detector, and the Fourier transform of the flux are shown for both the experiment and the simulation. The simulation reproduces the gross frequency and depth of the modulation present in the observed electron flux. However, since the phases of the measured waves and other profile parameters are unknown, the simulation cannot be expected to reproduce the particle flux exactly.

In summary, radial transport driven by drift-resonant fluctuations has been observed in a laboratory terrella experiment when the spectral characteristics of the observed fluctuations meet the conditions for chaotic particle motion. Strong modulation in the observed electron flux is reproduced in a numerical transport simulation.

We would like to acknowledge the advice of Akira Hasegawa during the design of CTX and recognize the contributions of R. Singer and R. Maruyama. This work was supported by AFOSR Grant No. F4A96209310071, NASA Grant No. NAGW-3539, and NSF Grant No. ATM-91–11396.

[1] M. Shulz and L. J. Lanzerotti, *Particle Diffusion in the Radiation Belts* (Springer-Verlag, New York, 1974).
[2] M. P. Nakada and G. D. Mead, J. Geophys. Res. **70**, 4777 (1965).
[3] T. A. Farley, A. D. Tomassain, and M. Walt, Phys. Rev. Lett. **25**, 47 (1970).
[4] A. Chan, L. Chen, and R. White, Geophys. Res. Lett. **16**, 1133 (1989).
[5] A. B. Rechester and R. B. White, Phys. Rev. Lett. **44**, 1586 (1980).
[6] M. W. Chen, L. R. Lyons, and M. Schulz, J. Geophys. Res. **99**, 5745 (1994).
[7] C. T. Hsu *et al.*, Phys. Rev. Lett. **72**, 2503 (1994).
[8] M. Mauel, H. Warren, and A. Hasegawa, IEEE Trans. Plasma Sci. **20**, 626 (1992).
[9] N. A. Krall, Phys. Fluids **9**, 820 (1966).
[10] H. L. Berk, Phys. Fluids **19**, 1255 (1976).
[11] K. Schindler, Rev. Geophys. **7**, 51 (1969).
[12] V. D. Il'in and A. N. Il'ina, Sov. Phys. JETP **43**, 661 (1976); **45**, 514 (1977).
[13] H. P. Warren, A. Bhattacharjee, and M. E. Mauel, Geophys. Res. Lett. **19**, 941 (1992).
[14] For example, R. A. Dandl *et al.*, Nucl. Fusion **4**, 344 (1964), or H. Ikegami *et al.*, Phys. Rev. Lett. **19**, 778 (1967).
[15] S. Hiroe *et al.*, Phys. Fluids **27**, 1019 (1984).
[16] L. J. Lanzerotti, C. S. Roberts, and W. L. Brown, J. Geophys. Res. **72**, 5893 (1967).
[17] A. H. Boozer, Phys. Fluids **9**, 904 (1980).
[18] A. G. Kornienko *et al.*, Phys. Lett. A **158**, 398 (1991).